Quantum Dot-Sensitized Hierarchical Micro/Nanowire Architecture for Photoelectrochemical Water Splitting

Wenjun Sheng,[†,‡] Bo Sun,[†,‡] Tielin Shi,[†] Xianhua Tan,[†] Zhengchun Peng,[§,*] and Guanglan Liao[†,*]

[†]State Key Laboratory of Digital Manufacturing Equipment and Technology, Huazhong University of Science and Technology, Wuhan 430074, China and [§]Technology Manufacturing Group, Intel Corporation, 2501 NW 229th Avenue, Hillsboro, Oregon 97124, United States. [‡]W. Sheng and B. Sun contributed equally to this work.

ABSTRACT We report the fabrication of quantum dot-sensitized hierarchical structure and the application of the structure as a photoanode for photoelectrochemical water splitting. The structure is synthesized by hydrothermally growing ZnO nanowires on silicon microwires grown with the vapor—liquid—solid method. Then the hierarchical structure is further sensitized with CdS and CdSe quantum dots and modified with IrO_x quantum dots. As a result, the silicon microwires, ZnO nanowires, and the quantum dot/ZnO core/shell structure form a multiple-level hierarchical heterostructure, which is remarkably beneficial for light absorption and charge carrier separation. Our experimental results reveal that the photocurrent density of our multiple-level hierarchical structure achieves a surprising 171 times enhancement compared to that from simple ZnO nanowires on a planar substrate. In addition, the photoanode shows high stability during the water-splitting experiment. These results prove that the quantum dot-sensitized hierarchical structure is an ideal candidate for a photoanode in solar water splitting applications. Importantly, the modular design approach we take to produce the photoanode allows for the integration of future discoveries for further improvement of its performance.

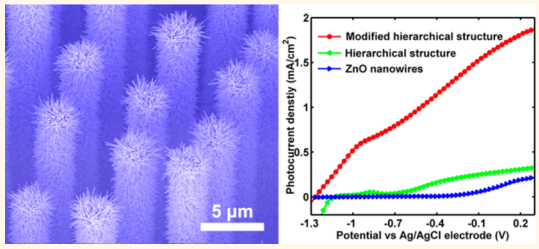

KEYWORDS: silicon microwires · ZnO nanowires · CdS · CdSe · IrO_x · photoelectrochemical water splitting

Due to the growing global energy demand and increasing concern for environmental issues, hydrogen has drawn considerable interest as a future energy carrier since it is a clean fuel with zero harmful byproducts after combustion.[1,2] Photoelectrochemical (PEC) water splitting under solar illumination has been regarded as one of the most attractive approaches to produce hydrogen, given that the production process is simple and environmentally friendly.[3,4]

Solar conversion efficiency and the stability of water splitting are mainly determined by the semiconducting material properties of the photoelectrodes.[5,6] Metal oxides such as TiO_2, Fe_2O_3, and ZnO have drawn more and more attention in this area.[7−10] Due to its high electron mobility,[11] ZnO has been investigated extensively for various energy conversion devices.[12−15] However, its conversion efficiency for water splitting is still low due to its large band gap.[8,9] On the other hand, the commonly used semiconductor silicon can absorb sunlight efficiently. Silicon wire arrays have been demonstrated to be efficient in photovoltaic cells and photoelectrochemical cells.[16−18] Furthermore, three-dimensional tree-like branched wires, especially the heterostructure, offer long optical paths for efficient light absorption, high-quality one-dimensional conducting channels for rapid charge transport, and high surface areas for fast electrochemical reactions, as well as easy integration of two or more materials to form the Z-scheme.[19,20] For instance, Si/TiO_2, Si/InGaN, and Si/ZnO hierarchical nanowire arrays have been demonstrated with drastically higher efficiency than one-dimensional nanowires.[20−22]

Recently, researchers have started employing narrow band gap semiconductors such as CdS, CdSe, and PbS in quantum dot-sensitized photoelectrochemical solar cells and achieved remarkable enhancement in efficiency.[23−25] However, the use of CdS and CdSe quantum dots is still limited by the upsetting challenge of photochemical

* Address correspondence to (G. Liao) guanglan.liao@hust.edu.cn, (Z. Peng) pengzhengchun@gmail.com.

Received for review April 16, 2014 and accepted June 18, 2014.

Published online June 18, 2014
10.1021/nn502121t

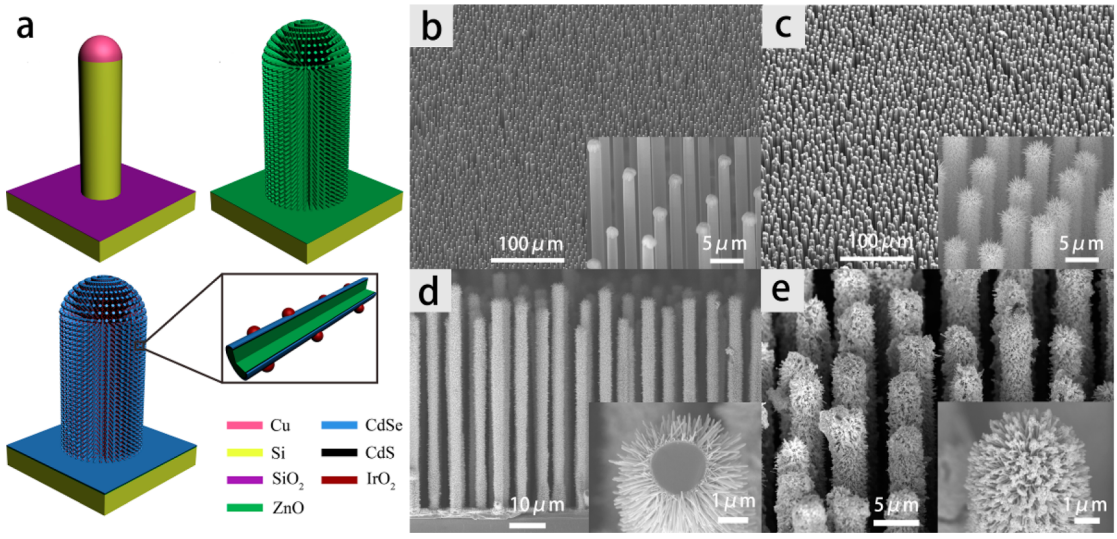

Figure 1. (a) Schematic of the photoanode fabrication process. Silicon microwire is grown on a silicon substrate, and ZnO nanowires are grown on the microwire, forming the Si/ZnO hierarchical structure. The structure is then sensitized with CdS and CdSe quantum dots in sequence and further modified with IrO_x quantum dots. The inset illustrates the core–shell characteristics of an ultimate nanowire. (b) SEM image of a silicon microwire array grown on a Si substrate. The inset is a magnified image in which the Cu catalyst can be seen clearly on the tip of microwires. (c) SEM image of the Si/ZnO hierarchical wire array where the inset is a magnified image for the hierarchical wires. (d) Sectional view of the Si/ZnO hierarchical wires where the inset shows a cracked wire. (e) SEM image of the ultimate quantum dot-sensitized hierarchical wires. The colloid paste coated on the surface can be clearly seen in the inset.

stability. Cadmium chalcogenide quantum dots have a relatively slower interfacial hole transfer rate compared to electron injection into metal oxides, thus causing the hole-induced anodic corrosion of cadmium chalcogenides.[26] Both the ZnS coating layer and IrO_x quantum dot modification were demonstrated as effective approaches to battle the corrosion.[27,28]

In this paper we propose a new kind of quantum dot-sensitized hierarchical micro/nanowire photoanode for PEC water splitting by integrating several critical components in the photoanode. We fabricate hierarchical structures by growing ZnO nanowires with a hydrothermal method on silicon microwires, which are grown using a vapor–liquid–solid (VLS) method. Then the hierarchical structures are co-sensitized with CdS and CdSe quantum dots and modified with IrO_x quantum dots. Although the relative band positions of ZnO, CdS, and CdSe in bulk phase are not seen as promising for this application, when these components are brought into direct contact, the band edges would be rearranged due to Fermi level alignment.[24,29] Considering the synergistic effect, we sensitize the hierarchical structure with CdS quantum dots first, followed by CdSe quantum dot sensitization. Consequently, the ZnO, CdS, and CdSe core–shell structures display an ideal stepwise band edge structure, which is remarkably advantageous in transporting photoexcited electrons and holes in the electrode. The ultimate photoanode produced in this way shows surprising enhancement of photocurrent density and efficiency compared to simple ZnO nanowire-based photoanodes.

RESULTS AND DISCUSSION

The photoanode fabrication process is schematically illustrated in Figure 1a. The silicon microwires are grown with the VLS method in a homemade chemical vapor deposition (CVD) equipment. The hierarchical structure is obtained by hydrothermally growing ZnO nanowires on silicon microwires. Then the structure is sensitized with CdS and CdSe quantum dots and modified with IrO_x quantum dots. The inset illustrates the core–shell characteristics of an ultimate quantum dot-sensitized ZnO nanowire. A series of scanning electron microscopy (SEM) images in Figure 1b–e depict the morphology of the photoanode after different fabrication steps. Figure 1b shows the tilted view of the silicon microwires grown by the VLS method, which are hexagonally and uniformly distributed on the substrate. The Cu catalyst on the top of the wires is seen in the magnified image (inset). Figure 1c and d display the tilted view and sectional view of the tree-like Si/ZnO hierarchical structure. The inset of Figure 1c is a magnified image of the hierarchical wires, while the inset of Figure 1d presents an accidentally cracked hierarchical wire, from which we can tell the density of the ZnO nanowire grown on the Si microwire is extremely high. Figure 1e shows the photoanode after the sensitization of three different quantum dots. We can clearly see a layer of colloid paste covering the surface of the hierarchical wires. The optical images shown in Figure S1 indicate the color change of the hierarchical structure after each quantum dot sensitization step. The diameter and height of the microwires

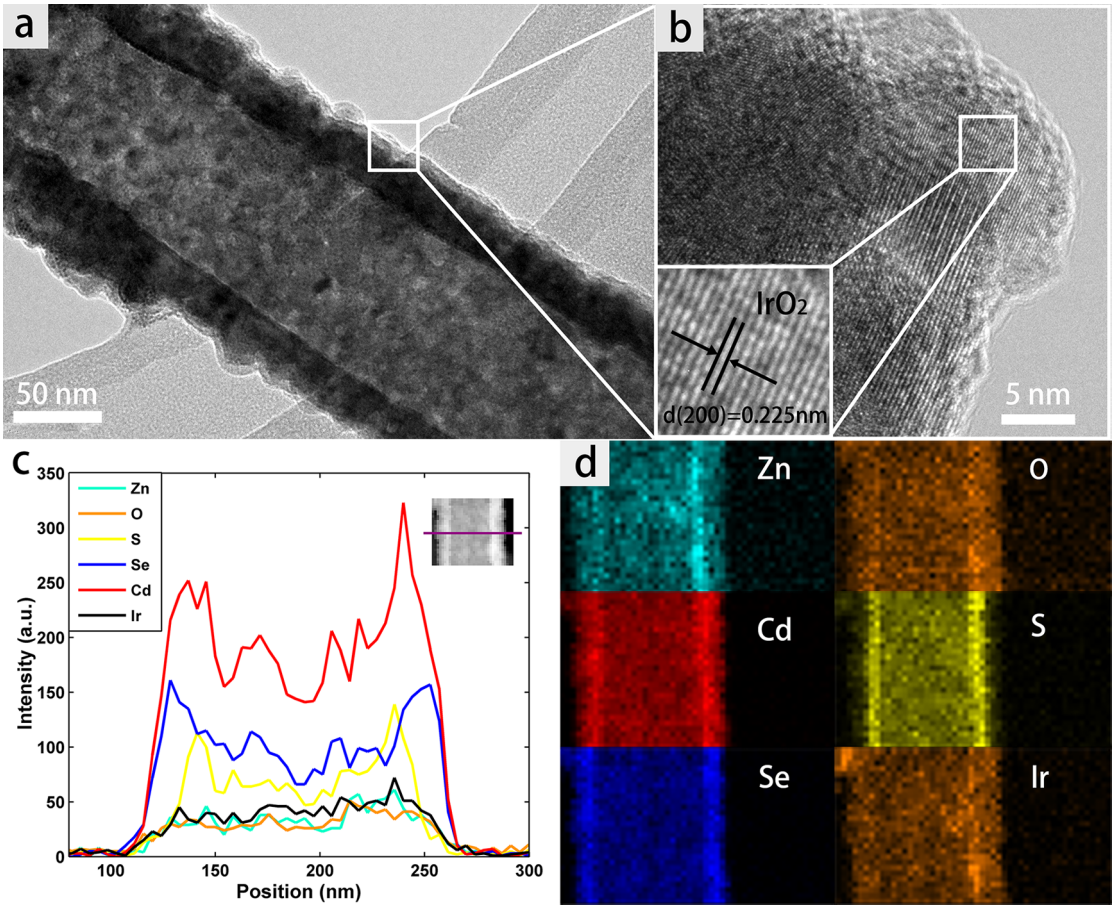

Figure 2. (a) TEM image of quantum dot-sensitized ZnO nanowire. (b) High-resolution TEM image collected from the edge of the nanowire. (c) Line scan profile of EDX spectra acquired across the core−shell structure as shown in the inset (HAADF scanning TEM image). (d) Elemental mappings of Zn, O, Cd, S, Se, and Ir acquired from the core−shell structure.

are about 2 and 70 μm, respectively. The ZnO nanowires grown on the surface of the silicon microwires are about 1.5 μm in length and 80 nm in diameter.

Transmission electron microscopy (TEM) images and energy dispersive X-ray (EDX) spectra of the quantum dot-sensitized ZnO nanowire are displayed in Figure 2. Figure 2a reveals a layer of shell about 30 nm thick wrapping the surface of the ZnO nanowire. A high-resolution TEM image (Figure 2b) collected from the boundary of the nanowire indicates that the shell has a polycrystalline structure, and a crystal grain on the edge of the shell has an interplanar spacing of 0.225 nm, which corresponds to a *d*-spacing of (200) planes of IrO_2. TEM characterization was carried out at each quantum dot sensitization step. The TEM image of CdS-sensitized ZnO nanowire (Figure 2Sa) displays a thin shell of several nanometers thick covering the ZnO nanowire, and the high-resolution TEM image (Figure 2Sb) displays an interplanar spacing of 0.28 nm, corresponding to the *d*-spacing of (200) planes of CdS. The TEM image of a CdS/CdSe-co-sensitized ZnO nanowire (Figure 2Sc) shows a thicker shell covering the nanowire, where the interplanar spacing of 0.33 nm in the outer layer is attributed to the (101) planes of CdSe (Figure 2Sd). Figure 2c shows the line scan profile of EDX spectra acquired along a line crossing the nanowire as shown in the inset (HAADF scanning TEM image). The intensity of the curves provides the evidence that the ZnO nanowires and CdS, CdSe, and IrO_2 quantum dots do form a core−shell structure with multiple shells. Figure 2d displays the elemental mappings of Zn, O, Cd, S, Se, and Ir, and the color intensity further confirms the core−shell morphology.

To determine the surface composition and chemical states of the photoanode, X-ray photoelectron spectroscopy (XPS) spectra were collected (Figure 3). The XPS peaks (Figure 3a) at about 1022 and 1041 eV correspond to the Zn $2p_{3/2}$ and Zn $2p_{1/2}$ states, and the XPS peak at about 531.8 eV (Figure 3b) corresponds to the O 1s state. The two peaks at 405.4 and 412.2 eV (Figure 3c) are in accord with the Cd $3d_{5/2}$ and Cd $3d_{3/2}$ states. The peaks depicted in Figure 3d and e at about 166 and 54.1 eV can be attributed to the S 2p and Se 3d states, respectively, and the two peaks in Figure 3f at 62.5 and 65.5 eV correspond to the Ir $4f_{7/2}$ and $4f_{5/2}$ states, respectively. Quantitative analysis of the spectra reveals that the surface of the photoanode contains 0.8% Zn, 42.39% O, 26.64% Cd, 4.47% S, 15.22% Se, and 10.44% Ir (atomic percentage, Table S1). Besides, we note significant noise in Figure 3a and some noise

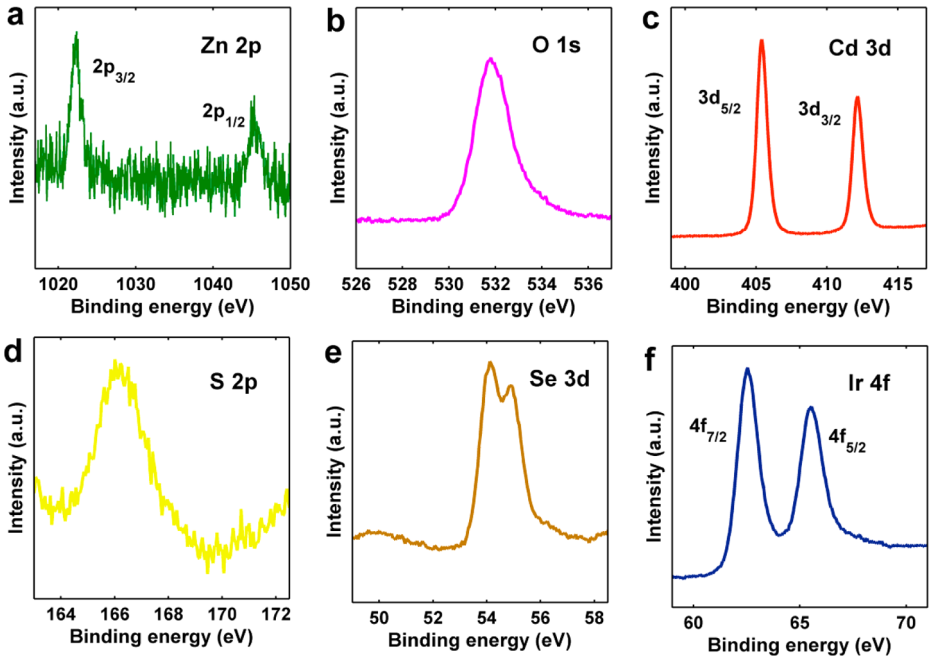

Figure 3. XPS spectra: (a) Zn 2p, (b) O 1s, (c) Cd 3d, (d) S 2p, (e) Se 3d, and (f) Ir 4f.

in Figure 3d. We believe this is due to ZnO core material being buried inside three layers of quantum dot shell structure, among which the CdS layer is the innermost. As such, the main surface compositions of the ultimate quantum dots loaded hierarchical wires are CdSe and IrO_x. Only in locations where the CdSe and IrO_x layers are thin can one obtain the spectra of Zn and S,[30,31] as shown in Figure 3a and d. These results further confirm the core−shell characteristics of the quantum dot-sensitized ZnO nanowires.

We investigated the photocatalytic activities of the photoanodes with different structures and components for PEC water splitting. Figure 4a illustrates the schematic of the water splitting process in the PEC cell and the energy band distribution of different components used in our hierarchical structure. The stepwise band edge structure should produce a significant synergy for efficient transport of photoexcited electrons and holes in the electrode.[29] An aqueous solution of Na_2S and Na_2SO_3 is used as an electrolyte as well as a sacrificial reagent to maintain the stability of the CdSe quantum dots in the photoelectrochemical cell.[28] Although the polysulfide redox couples (S^{2-}/S_n^{2-}) are quite effective in scavenging the holes from CdSe, the decline of the photocurrent is also an inevitable problem.[26,32] Since cadmium chalcogenide quantum dots have relatively slower interfacial hole transfer kinetics as compared to electron injection into metal oxide, the holes gradually accumulate within quantum dots and promote hole-induced anodic corrosion.[26,28,32] To overcome this issue, we modify the surface with an oxygen evolution catalyst, IrO_x, which should substantially improve the photochemical stability.

Photoexcited electrons at CdSe/CdS quantum dots and the Si/ZnO hierarchical structure are first collected on the bottom electrode *via* the Si/ZnO hierarchical structure, which also works as the main channel for charge carrier transport. The photoexcited electrons then move to the Pt counter electrode *via* an external circuit and generate hydrogen once they arrive at the Pt surface. On the other hand, the photoexcited holes in the hierarchical structure flow through the channel, arrive at the electrode surface accompanying the holes from CdS and CdSe, converge at the IrO_x quantum dots, and then are scavenged by polysulfide redox couples.

Figure 4b displays the line sweep voltammograms measured from ZnO nanowires grown on the planar Si substrate, Si/ZnO hierarchical wire arrays, and quantum dot-sensitized Si/ZnO hierarchical wire arrays, where the inset shows the magnified view of the data within the dotted box. The photocurrent density of ZnO nanowires is about 0.0066 and 0.098 mA/cm^2 at the potential of −0.4 and 0 V *versus* Ag/AgCl, while the value for the Si/ZnO hierarchical structure increases to 0.157 and 0.27 mA/cm^2, about 24 times and 3 times enhancement, respectively. After the sensitization of quantum dots the value reaches 1.13 and 1.64 mA/cm^2, corresponding to 171 times and 17 times enhancement, respectively.

To quantitatively analyze the efficiency of the three different photoanodes for PEC water splitting, the photoconversion efficiency is calculated from the line sweep voltammogram.[33] As shown in Figure 4c, the ZnO nanowire structure achieves an efficiency of 0.018% at 0 V *versus* Ag/AgCl, while the hierarchical structure achieves an efficiency of 0.08% at about −0.3 V *versus*

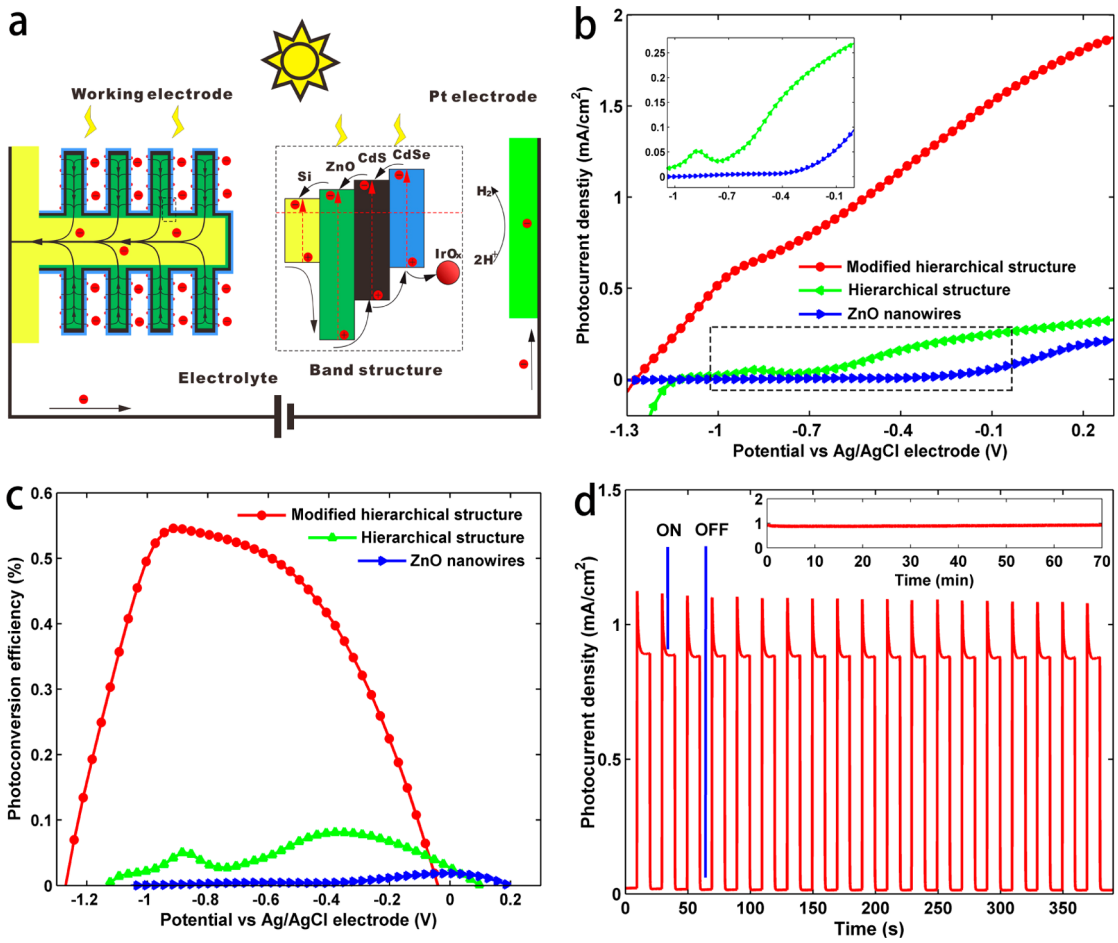

Figure 4. (a) Schematic of the water splitting process in the PEC cell and energy level distribution of different components. (b) Line sweep voltammograms measured from ZnO nanowires, Si/ZnO hierarchical wires, and quantum dot-sensitized Si/ZnO hierarchical wires, where the inset shows a magnified view of the data in the dotted box for comparison. (c) Photoconversion efficiency of three different samples calculated from the line sweep voltammograms. (d) Time-dependent photocurrent density of the quantum dot-sensitized photoanode at repeated on/off cycles of illumination. The inset shows a 70 min stable measurement result under successive illumination.

Ag/AgCl, and after sensitization with quantum dots the efficiency reaches 0.55% at −0.92 V *versus* Ag/AgCl, corresponding to 4.4 times and 30 times enhancement, respectively. In comparison, the photoconversion efficiency achieved in this work is much better than the latest advancement reported by similar research.[18,21,34]

To study the stability of our photoanode, time-dependent measurements have been carried out on the quantum dot-sensitized photoanode. With repeated on/off cycles of illumination from the solar simulator, the device displays a highly stable photocurerent density, about 0.9 mA/cm^2 at −0.6 V *versus* Ag/AgCl (Figure 4d). Measurement under successive illumination for 70 min reveals no obvious decay of photocurrent, which is substantially improved from previous research focusing on Si- and ZnO-based photoanodes.[15,22,35] In general, as the photoelectrode material, ZnO is severely limited by chemical instability under both anodic and cathodic bias.[36] It has been reported that the working lifetime of PEC cells using ZnO nanorods grown on planar silicon as photoanodes is only a few minutes.[35] We attribute the high stability of our photoanodes to the multiple shell structure of the quantum dots. As a result, our photoanode based on quantum dot-sensitized Si/ZnO hierarchical wire arrays possesses high potential for PEC water splitting, as both the structural integrity and chemical stability are critical factors in this application.

CONCLUSIONS

In summary, we have successfully fabricated a new kind of quantum dot-sensitized three-dimensional hierarchical structure for photoelectrochemical water splitting. The tree-like structure has a large surface area, which significantly increases the contact area to the electrolyte and substantially promotes the photoelectrochemical reactions. The core−shell structure of the nanowire branches has advantages in the separation and collection of the electron−hole pairs, and the hierarchical wires' backbone works as the carrier transfer channel. Our experimental results reveal that the photocurrent density and efficiency of the Si/ZnO

hierarchical structure achieves 23- and 4.4-fold enhancement, respectively, compared to similar ZnO nanowires on a planar substrate. With the quantum dot sensitization, the ultimate hierarchical structure achieves a strikingly high performance, *i.e.*, 171- and 30-fold enhancement in photocurrent density and conversion efficiency, respectively. Besides, the quantum dot-sensitized hierarchical structure has demonstrated high stability during the water splitting. These results prove that the quantum dot-sensitized hierarchical micro/nanowire architecture is an ideal candidate to construct a photoanode for water splitting. Also demonstrated in this work is the successful attempt of modular design and fabrication for energy conversion devices.

EXPERIMENTAL SECTION

Photoanode Preparation. To grow silicon microwires, an n-type Si(111) wafer with a 450 nm oxide layer was used as the substrate. Hexagonally distributed circular holes with 3 μm diameter and 7 μm space were photolithographically defined on the substrate. The substrate was etched in buffered hydrofluoric acid (BHF) to transfer the pattern to the oxide layer. A copper layer about 400 nm thick was sputtered on the substrate to form the growth seeds in the pattern. After that the substrate was placed into a homemade atmospheric pressure chemical vapor deposition (APCVD) equipment to grow silicon microwires by the VLS method.[37] The substrate was first annealed at 1050 °C with 500 sccm H_2 for 20 min, followed by silicon microwire growth with 500 sccm H_2 and 15 sccm $SiCl_4$ at 1050 °C for 20 min. The silicon microwires were doped with phosphorus using diffusion wafers (Saint Gobain, PH 900) for 80 min at 950 °C in N_2 flows. The phosphorosilicate glass formed on the surface of the silicon microwires was etched off by diluted HF (5%). To remove Cu catalyst the silicon microwires were first etched with RCA2 ($H_2O/HCl/H_2O_2$ = 6:1:1) at 70 °C for 1 h and then etched with diluted HF for about 3 min. After that the high surface area Si/ZnO hierarchical wires were formed by hydrothermally growing ZnO nanowires on the silicon microwires. To further enhance the photocatalytic activity and stability, the hierarchical wires were sensitized with CdS and CdSe quantum dots by successive ion layer adsorption and reaction (SILAR) and the chemical bath deposition (CBD) method, respectively, and finally modified with IrO_x quantum dots by immersing the sample into an IrO_x colloid solution.

In a typical SILAR deposition cycle for CdS, the hierarchical wires were immersed in the 100 mM $CdSO_4$ aqueous solution (cation precursor) for 30 s and rinsed with deionized (DI) water to remove excess ions that were weakly bound to the nanowire surfaces; then the hierarchical wires were immersed in the 100 mM Na_2S aqueous solution (anion precursor) for 30 s and rinsed with DI water again. This deposition process was repeated for about 20 cycles to get a suitable thickness of CdS shell on the ZnO nanowires. For the deposition of CdSe, the as-prepared CdS-sensitized hierarchical wires were immersed in an aqueous solution containing $Cd(CH_3COO)_2/Na_2SeSO_3/NH_4OH$ = 2.5 mM/2.5 mM/45 mM for 3 h at 95 °C. This procedure was repeated three times to obtain moderate CdSe loading on the CdS/ZnO nanowires.

To prepare the colloidal IrO_x solution, the pH of a 2 mM Na_2IrCl_6 solution was adjusted to 13 by adding NaOH. The color of the solution then changed from yellow to blue by heating at 90 °C for 20 min. The colored solution was cooled by immersion in an ice bath, and the pH of the solution was tuned to 1 by rapidly adding HNO_3. Then the solution was stirred for about 80 min for sufficient acid condensation. After regulating the pH of the solution to 6.8, the CdS and CdSe quantum dot cosensitized hierarchical wires were immersed in the IrO_x colloidal solution for 3 h to adsorb the IrO_x quantum dots. Then, the as-prepared electrode was washed with DI water and dried at 100 °C in the atmosphere for 12 h.

Photoanode Characterization and Measurements. The morphology of the photoelectrode was observed by a field emission scanning electron microscope (JSM-7600F, JEOL), and the detailed microscopic structure and element composition were observed by a field emission transmission electron microscope (Tecnai G2 F30, FEI) combined with an energy-dispersive X-ray spectrometer. An X-ray photoelectron spectrometer (Axis Ultra DLD, Shimadzu) equipped with a monochromatic Al Kα source (1486.6 eV) was employed to determine the surface chemical composition and states of the ultimate quantum dot-sensitized hierarchical structure. All the XPS spectra were obtained in the constant pass energy mode, where the pass energy of the analyzer was set at 20 eV. Here the binding energy of the C 1s peak (285 eV) arising from adventitious carbon was used for the energy calibration.

For PEC water splitting, the back of the photoelectrode was etched with diluted HF (5%), covered with a layer of silver paste, and then connected to Cu wires using tin soldering. After that, the electrode was sealed with polydimethylsiloxane , in which only a well-defined area of the front side was exposed to the electrolyte. The photoelectrochemical measurements were performed using a typical three-electrode potentiostat system (Autolab PGSTAT302N, Metrohm Autolab) with a Pt counter electrode and a Ag/AgCl reference electrode. The solar simulator (Oriel 94043A, Newport) with a light intensity of 100 mW/cm^2 was used as the light source. The electrolyte contains a 0.25 M Na_2S and 0.35 M Na_2SO_3 aqueous solution.

Conflict of Interest: The authors declare no competing financial interest.

Acknowledgment. The authors are grateful for the financial support by the National Natural Science Foundation of China (Grant Nos. 51175210 and 51222508).

Supporting Information Available: Optical images obtained by optical microscope, additional TEM images of quantum dot-sensitized nanowires, and quantification report of the XPS experiment. This material is available free of charge *via* the Internet at http://pubs.acs.org.

REFERENCES AND NOTES

1. Zou, Z.; Ye, J.; Sayama, K.; Arakawa, H. Direct Splitting of Water under Visible Light Irradiation with an Oxide Semiconductor Photocatalyst. *Nature* **2001**, *414*, 625–627.
2. Davis, S. J.; Caldeira, K.; Matthews, H. D. Future CO_2 Emissions and Climate Change from Existing Energy Infrastructure. *Science* **2010**, *329*, 1330–1333.
3. Paracchino, A.; Laporte, V.; Sivula, K.; Grätzel, M.; Thimsen, E. Highly Active Oxide Photocathode for Photoelectrochemical Water Reduction. *Nat. Mater.* **2011**, *10*, 456–461.
4. Chen, Y. W.; Prange, J. D.; Dühnen, S.; Park, Y.; Gunji, M.; Chidsey, C. E. D.; McIntyre, P. C. Atomic Layer-Deposited Tunnel Oxide Stabilizes Silicon Photoanodes for Water Oxidation. *Nat. Mater.* **2011**, *10*, 539–544.
5. Schrauben, J. N.; Hayoun, R.; Valdez, C. N.; Braten, M.; Fridley, L.; Mayer, J. M. Titanium and Zinc Oxide Nanoparticles Are Proton-Coupled Electron Transfer Agents. *Science* **2012**, *336*, 1298–1301.
6. Tachibana, Y.; Vayssieres, L.; Durrant, J. R. Artificial Photosynthesis for Solar Water-Splitting. *Nat. Photonics* **2012**, *6*, 511–518.
7. Cho, I. S.; Chen, Z. B.; Forman, A. J.; Kim, D. R.; Rao, P. M.; Jaramillo, T. F.; Zheng, X. L. Branched TiO_2 Nanorods for Photoelectrochemical Hydrogen Production. *Nano Lett.* **2011**, *11*, 4978–4984.
8. Lin, Y. J.; Zhou, S.; Sheehan, S. W.; Wang, D. W. Nanonet-Based Hematite Heteronanostructures for Efficient Solar Water Splitting. *J. Am. Chem. Soc.* **2011**, *133*, 2398–2401.

9. Ahn, K. S.; Yan, Y.; Shet, S.; Jones, K.; Deutsch, T.; Turner, J.; Al-Jassim, M. ZnO Nanocoral Structures for Photoelectrochemical Cells. *Appl. Phys. Lett.* **2008**, *93*, 163117.
10. Ladanov, M.; Ram, M. K.; Matthews, G.; Kumar, A. Structure and Opto-Electrochemical Properties of ZnO Nanowires Grown on n-Si Substrate. *Langmuir* **2011**, *27*, 9012–9017.
11. Yin, Z.; Wang, Z.; Du, Y.; Qi, X.; Huang, Y.; Xue, C.; Zhang, H. Full Solution-Processed Synthesis of All Metal Oxide-Based Tree-like Heterostructures on Fluorine-Doped Tin Oxide for Water Splitting. *Adv. Mater.* **2012**, *24*, 5374–5378.
12. Xue, X.; Nie, Y.; He, B.; Xing, L.; Zhang, Y.; Wang, Z. L. Surface Free-Carrier Screening Effect on the Output of a ZnO Nanowire Nanogenerator and Its Potential as a Self-Powered Active Gas Sensor. *Nanotechnology* **2013**, *24*, 225501.
13. Yang, P.; Xiao, X.; Li, Y.; Ding, Y.; Qiang, P.; Tan, X.; Mai, W.; Lin, Z.; Wu, W.; Li, T.; Jin, H.; Liu, P.; Zhou, J.; Wong, C. P.; Wang, Z. L. Hydrogenated ZnO Core-Shell Nanocables for Flexible Supercapacitors and Self-Powered Systems. *ACS Nano* **2013**, *7*, 2617–2626.
14. Yang, Y.; Zhang, H.; Zhu, G.; Lee, S.; Lin, Z. H.; Wang, Z. L. Flexible Hybrid Energy Cell for Simultaneously Harvesting Thermal, Mechanical, and Solar Energies. *ACS Nano* **2013**, *7*, 785–790.
15. Yang, Y.; Zhang, H.; Lin, Z. H.; Liu, Y.; Chen, J.; Lin, Z.; Zhou, Y. S.; Wong, C. P.; Wang, Z. L. A Hybrid Energy Cell for Self-Powered Water Splitting. *Energy Environ. Sci.* **2013**, *6*, 2429–2434.
16. Kelzenberg, M. D.; Boettcher, S. W.; Petykiewicz, J. A.; Turner-Evans, D. B.; Putnam, M. C.; Warren, E. L.; Spurgeon, J. M.; Briggs, R. M.; Lewis, N. S.; Atwater, H. A. Enhanced Absorption and Carrier Collection in Si Wire Arrays for Photovoltaic Applications. *Nat. Mater.* **2010**, *9*, 239–244.
17. Boettcher, S. W.; Spurgeon, J. M.; Putnam, M. C.; Warren, E. L.; Turner-Evans, D. B.; Kelzenberg, M. D.; Maiolo, J. R.; Atwater, H. A.; Lewis, N. S. Energy-Conversion Properties of Vapor-Liquid-Solid—Grown Silicon Wire-Array Photocathodes. *Science* **2010**, *327*, 185–187.
18. Strandwitz, N. C.; Turner-Evans, D. B.; Tamboli, A. C.; Chen, C. T.; Atwater, H. A.; Lewis, N. S. Photoelectrochemical Behavior of Planar and Microwire-Array Si/GaP Electrodes. *Adv. Energy Mater.* **2012**, *2*, 1109–1116.
19. Grätzel, M. Photoelectrochemical Cells. *Nature* **2001**, *414*, 338–344.
20. Shi, J.; Hara, Y.; Sun, C.; Anderson, M. A.; Wang, X. Three-Dimensional High-Density Hierarchical Nanowire Architecture for High-Performance Photoelectrochemical Electrodes. *Nano Lett.* **2011**, *11*, 3413–3419.
21. Hwang, Y. J.; Wu, C. H.; Hahn, C.; Jeong, H. E.; Yang, P. Si/InGaN Core/Shell Hierarchical Nanowire Arrays and Their Photoelectrochemical Properties. *Nano Lett.* **2012**, *12*, 1678–1682.
22. Sun, K.; Jing, Y.; Li, C.; Zhang, X.; Aguinaldo, R.; Kargar, A.; Madsen, K.; Banu, K.; Zhou, Y.; Bando, Y.; Liu, Z.; Wang, D. 3D Branched Nanowire Heterojunction Photoelectrodes for High-Efficiency Solar Water Splitting and H_2 Generation. *Nanoscale* **2012**, *4*, 1515–1521.
23. Su, F.; Lu, J.; Tian, Y.; Ma, X.; Gong, J. Branched TiO_2 Nanoarrays Sensitized with CdS Quantum Dots for Highly Efficient Photoelectrochemical Water Splitting. *Phys. Chem. Chem. Phys.* **2013**, *15*, 12026–12032.
24. Lee, Y. L.; Chi, C. F.; Liau, S. Y. CdS/CdSe Co-Sensitized TiO_2 Photoelectrode for Efficient Hydrogen Generation in a Photoelectrochemical Cell. *Chem. Mater.* **2010**, *22*, 922–927.
25. Sheng, P.; Li, W.; Cai, J.; Wang, X.; Tong, X.; Cai, Q.; Grimesb, C. A. A Novel Method for the Preparation of a Photocorrosion Stable Core/Shell CdTe/CdS Quantum Dot TiO_2 Nanotube Array Photoelectrode Demonstrating an AM 1.5G Photoconversion Efficiency of 6.12%. *J. Mater. Chem. A* **2013**, *1*, 7806–7815.
26. Chakrapani, V.; Baker, D.; Kamat, P. V. Understanding the Role of the Sulfide Redox Couple (S^{2-}/S_n^{2-}) in Quantum Dot-Sensitized Solar Cells. *J. Am. Chem. Soc.* **2011**, *133*, 9607–9615.
27. Zewdu, T.; Clifforda, J. N.; Palomares, E. Synergistic Effect of ZnS Outer Layers and Electrolyte Methanol Content on Efficiency in TiO_2/CdS/CdSe Sensitized Solar Cells. *Phys. Chem. Chem. Phys.* **2012**, *14*, 13076–13080.
28. Seol, M.; Jang, J. W.; Cho, S.; Lee, J. S.; Yong, K. Highly Efficient and Stable Cadmium Chalcogenide Quantum Dot/ZnO Nanowires for Photoelectrochemical Hydrogen Generation. *Chem. Mater.* **2013**, *25*, 184–189.
29. Seol, M.; Kim, H.; Kim, W.; Yong, K. Highly Efficient Photoelectrochemical Hydrogen Generation Using a ZnO Nanowire Array and a CdSe/CdS Co-Sensitizer. *Electrochem. Commun.* **2010**, *12*, 1416–1418.
30. Dabbousi, B. O.; Rodriguez-Viejo, J.; Mikulec, F. V.; Heine, J. R.; Mattoussi, H.; Ober, R.; Jensen, K. F.; Bawendi, M. G. (CdSe)ZnS Core-Shell Quantum Dots: Synthesis and Characterization of a Size Series of Highly Luminescent Nanocrystallites. *J. Phys. Chem. B* **1997**, *101*, 9463–9475.
31. Hsu, S. H.; Hung, S. F.; Chien, S. H. CdS Sensitized Vertically Aligned Single Crystal TiO_2 Nanorods on Transparent Conducting Glass with Improved Solar Cell Efficiency and Stability Using ZnS Passivation Layer. *J. Power Sources* **2013**, *233*, 236–243.
32. Bang, J. H.; Kamat, P. V. Quantum Dot Sensitized Solar Cells. A Tale of Two Semiconductor Nanocrystals: CdSe and CdTe. *ACS Nano* **2009**, *3*, 1467–1476.
33. Khan, S. U. M.; Al-Shahry, M.; Ingler, W. B., Jr. Efficient Photochemical Water Splitting by a Chemically Modified n-TiO_2. *Science* **2002**, *297*, 2243–2245.
34. Liu, C.; Tang, J.; Chen, H. M.; Liu, B.; Yang, P. A Fully Integrated Nanosystem of Semiconductor Nanowires for Direct Solar Water Splitting. *Nano Lett.* **2013**, *13*, 2989–2992.
35. Wei, Y.; Ke, L.; Leong, E. S. P.; Liu, H.; Liew, L. L.; Teng, J. H.; Du, H.; Sun, X. W. Enhanced Photoelectrochemical Performance of Bridged ZnO Nanorods Arrays Grown on V-Grooved Structure. *Nanotechnology* **2012**, *23*, 365704.
36. Osterloh, F. E. Inorganic Nanostructures for Photoelectrochemical and Photocatalytic Water Splitting. *Chem. Soc. Rev.* **2013**, *42*, 2294–2320.
37. Kayes, B. M.; Filler, M. A.; Putnam, M. C.; Kelzenberg, M. D.; Lewis, N. S.; Atwater, H. A. Growth of Vertically Aligned Si Wire Arrays over Large Areas (>1 cm^2) with Au and Cu Catalysts. *Appl. Phys. Lett.* **2007**, *91*, 103110.